

III.4.3 Nuclear collisions at the LHC

John M. Jowett

GSI Helmholtzzentrum für Schwerionenforschung GmbH, Darmstadt, Germany
CERN, Geneva, Switzerland

III.4.3.1 Introduction

III.4.3.1.1 *Historical perspective*

A particle accelerator is invariably a substantial investment on the part of the community that it serves, be it a university laboratory, a hospital, an industrial plant, a national laboratory, or an essentially global laboratory like CERN. That investment must be secured by compelling motivation. For the highest-energy accelerators and colliders, that is invariably the prospect of significant discoveries in particle physics. For the LHC, initially conceived as a high-energy proton-proton collider, the most prominent of these was its potential to discover the Higgs boson (or refute the theory that predicted it). Despite the public perception, driven by the exclusive focus of much media coverage on that momentous discovery, the publication lists of the LHC experiments demonstrate that p–p collisions have yielded abundant solid science, and more will come.

Nevertheless, as with any accelerator, having made the initial investment, it is natural to ask what we, as accelerator physicists and engineers, can do to add scientific value? In this seminar, we consider the LHC as a case study in extending the capabilities of an accelerator. First, we need to look back at the history of hadron colliders.

Hadron colliders of the late 20th century were focused on elementary particle physics, so collided mainly protons and antiprotons, the *most elementary* hadronic entities available (CERN's ISR were very briefly an exception [1] to this rule). The 21st century opened with the first colliding beams of gold nuclei—some of the *least elementary* hadronic entities that one can hope to accelerate to high energies—at the Relativistic Heavy-Ion Collider (RHIC) at Brookhaven National Laboratory. A decade later, the LHC continued the programme by colliding lead nuclei at energies over an order of magnitude greater for the exploration of hadronic matter at extreme energy density and temperature.

Both hadron colliders currently operating are colliding beams of atomic nuclei (fully stripped heavy ions), and the active proposals for future hadron colliders, at very high and very low energies, all consider heavy-ion collisions. More remarkably still, although it was not always part of their initial ambitions, *all active experiments* at hadron colliders are now exploiting their complementary capabilities for heavy-ion physics.

The relative importance of beam-physics phenomena in limiting collider performance changes quite dramatically between operation with protons and heavy ions. I like to summarise this by saying that while the main performance limits for proton beams are generally related to the *high charge per*

This section should be cited as: Nuclear collisions at the LHC, J.M. Jowett, DOI: [10.23730/CYRSP-2024-003.1953](https://doi.org/10.23730/CYRSP-2024-003.1953), in: Proceedings of the Joint Universities Accelerator School (JUAS): Courses and exercises, E. Métral (ed.), CERN Yellow Reports: School Proceedings, CERN-2024-003, DOI: [10.23730/CYRSP-2024-003](https://doi.org/10.23730/CYRSP-2024-003), p. 1953.
© CERN, 2024. Published by CERN under the [Creative Commons Attribution 4.0 license](https://creativecommons.org/licenses/by/4.0/).

bunch of beam particles, effects related to the *high charge per beam particle* tend to dominate for heavy ions.

Within the space of this seminar, we can cover some, but by no means all, of this beam physics; a general review with many references can be found in Ref. [1].

Then we shall go on to give an outline of how the LHC's rich nuclear collision program has developed far beyond initial plans and expectations during Run 1 and Run 2. These runs have laid the foundations for still higher performance in Run 3 (now under way) and beyond.

We do not touch at all on the vast subject of the operation of the LHC injectors with heavy ions and how it determines the bunch filling patterns in the LHC. This review article [1] provides a general outline on ion colliders and their injectors and further information can be found in other lectures in this school and other citations below.

III.4.3.1.2 “Heavy-ion” physics—what is it about?

Recent reviews of the subject include [2, 3]. To quote Ref. [3],

We study heavy-ion collisions to gain insight into perhaps the simplest form of complex matter, described by the fundamental laws of Quantum Chromodynamics. This superhot liquid filled the microseconds-old Universe, making it the first complex matter to form as well as the source of all protons and neutrons. heavy-ion collisions are Little Bangs, recreating droplets of Big Bang matter.

Within a time of order of $1 \text{ fm}/c$, the matter and entropy produced in a heavy-ion collision form a droplet of strongly coupled QGP, evolving according to relativistic hydrodynamics with very small specific viscosity.

Quantum chromodynamics is the only sector of the Standard Model whose collective and thermodynamical behaviours are amenable to laboratory study and, not surprisingly, a wealth of interesting physical phenomena can be studied in heavy-ion collisions. Before the LHC started-up, RHIC experiments found that the deconfined Quark-Gluon Plasma (QGP) had the unanticipated properties of a strongly-coupled, almost perfect fluid. As foreseen, the higher temperatures ($\sim 10^{12}$ K or about 200 000 times the temperature at the core of the Sun), longer lifetime and more rapid equilibration of the QGP at the LHC allow studies with a broad spectrum of quark bound states as hard probes of this hot and ultra-dense matter. Unexpected phenomena, characteristic of collectivity in small systems were discovered in the first pilot fill of p–Pb collisions in 2012 (see below), and even in rare, high-multiplicity p–p collisions. Thermal production of the heaviest man-made anti-matter and hyper-matter nuclei is also observed.

Highly-charged, ultra-relativistic nuclei generate intense electromagnetic fields, equivalent to pulses of quasi-real photons with spectrum extending to hundreds of GeV at the LHC. Ultraperipheral collisions, where the impact parameter is too large for nuclear overlap ($b > 2R_A$), induce *photon-photon* and *photonuclear* interactions, with cross-sections depending on high powers of the nuclear charge Z . Besides creating a new class of collisional effects limiting collider performance (see below), these access a further range of high-energy phenomena beyond those associated with the QGP. A striking example is

the first observation by the ATLAS experiment of the long-anticipated elastic scattering of light by light. The LHC is therefore also, in a very real sense, a *photon-photon collider*

III.4.3.2 Nuclear beam physics

III.4.3.2.1 Energy, momentum and mass of heavy ions

The energy and momentum of heavy-ion or nuclear beams is quoted in different ways which we should clarify.

Consider a nucleus¹ of charge Ze , mass m and nucleon number (mass number) A . Its energy and momentum are related by the square of its 4-momentum vector $P = (E/c, \mathbf{p})$

$$P^2 = E^2/c^2 - p^2 = m^2c^2 \quad (\text{III.4.1})$$

to the Lorentz-invariant mass, m .

Traditionally, in low-energy ion accelerators, the *kinetic energy per nucleon* is quoted in parameter lists,

$$E_K = \frac{\sqrt{p^2c^2 + m^2c^4} - mc^2}{A} \approx \frac{E}{A}, \quad (\text{III.4.2})$$

but it is important to remember that this quantity does not appear in any equation of motion! My personal rule is to avoid confusion by never using any kind of “energy per nucleon” in beam physics calculations. It can be quoted at the end if required.

At the LHC, where the $^{208}\text{Pb}^{82+}$ beams are ultra-relativistic, we adopt the convention of quoting the energy as, e.g.,

$$E \approx pc = \underbrace{7.0 Z \text{ TeV}}_{\text{Energy per charge}} = \underbrace{2.76 A \text{ TeV}}_{\text{Energy per nucleon}} = \underbrace{574 \text{ TeV}}_{\text{Energy of the nucleus}}. \quad (\text{III.4.3})$$

The $7.0 Z \text{ TeV}$ form is convenient in practice as it indicates that the magnetic fields in the ring are the same as those for a proton beam of energy $E_p \simeq p_p c = 7.0 \text{ TeV}$. The second form gives the traditional “energy per nucleon” and the third is simply the energy of a single particle (a nucleus) in the beam.

In precise calculations, such as those relating to RF frequencies, it is also important to use the correct mass of a nucleus. For the case of the $^{208}\text{Pb}^{82+}$ nucleus (with $Z = 82$, $A = 208$) most commonly accelerated in the LHC, standard reference tables provide the mass of the neutral atom of this isotope (in atomic mass units or dalton) so we have to subtract the mass of the electrons²

$$m = 207.977u - 82m_e \quad (\text{III.4.4})$$

$$= (193.729 - 82 \times 0.000511) \text{ GeV}/c^2 \quad (\text{III.4.5})$$

$$= 193.687 \text{ GeV}/c^2. \quad (\text{III.4.6})$$

It is common to approximate this by simply scaling the proton mass by the nucleon number, which

¹For partially stripped ions in earlier stages of the LHC injector chain, Z should be replaced by the charge state Q .

²In principle we should also subtract the binding energy of the electrons but this is $< 1 \text{ MeV}$.

neglects the nuclear binding energy,

$$Am_p = 208m_p = 195.161 \text{ GeV}/c^2. \quad (\text{III.4.7})$$

While convenient, this is as crude approximation to the nuclear mass. To retain its convenience, we can, where appropriate, make the substitution

$$A \rightarrow A_p = m/m_p = 206.43 \text{ for the } {}^{208}\text{Pb}^{82+} \text{ case.} \quad (\text{III.4.8})$$

III.4.3.2.2 Kinematics of nuclear collisions

Let us consider the collisions of nuclei of charges Z_1 and Z_2 in rings with magnetic field set for protons of momentum p_p . The momenta of these nuclei are therefore $Z_1 p_p$ and $Z_2 p_p$. This corresponds to the configuration of the LHC where the two-in-one magnet design imposes equal and opposite bending magnetic fields in the two apertures even if the two colliding species are different. As we shall see later, the LHC has collided protons with Pb nuclei.

Recall that the rapidity of a particle with velocity v is defined as $y = \tanh^{-1}(v/c)$.

It is straightforward to show that the centre-of-mass energy, longitudinal head-on³ collisions of the two nuclei are

$$\sqrt{s} = (P_1 + P_2)^2 \approx 2c p_p \sqrt{Z_1 Z_2} \quad (\text{III.4.9})$$

$$\frac{v_{\text{CM}}}{c} = \frac{(\mathbf{p}_1 + \mathbf{p}_2)c}{(E_1 + E_2)} \approx \frac{Z_1 - Z_2}{Z_1 + Z_2} \quad (\text{III.4.10})$$

$$y_{\text{CM}} = \tanh^{-1} \frac{v_{\text{CM}}}{c} = \frac{1}{2} \log \frac{Z_1}{Z_2} \quad (\text{III.4.11})$$

On the other hand, the average centre-of-mass energy, longitudinal velocity and rapidity in the collisions *between two nucleons within the nuclei* are

$$\sqrt{s_{\text{NN}}} \approx 2c p_p \sqrt{\frac{Z_1 Z_2}{A_1 A_2}} \quad (\text{III.4.12})$$

$$\frac{v_{\text{NN}}}{c} \approx \frac{Z_1/A_1 - Z_2/A_2}{Z_1/A_1 + Z_2/A_2} \quad (\text{III.4.13})$$

$$y_{\text{NN}} \approx \frac{1}{2} \log \frac{Z_1 A_2}{Z_2 A_1} \quad (\text{III.4.14})$$

It is important to understand physically why v_{CM} and v_{NN} are of opposite sign.

The collision energy customarily quoted for heavy-ion collisions is $\sqrt{s_{\text{NN}}}$, the *energy per colliding nucleon pair*. Two of the LHC experiments (ALICE and LHCb) are asymmetric along the collision axis and reversing the direction of unequal beams (e.g., in proton-lead collisions, with $y_{\text{NN}} \approx 0.465$) allows them to access collision products in different rapidity regions in the laboratory frame.

³Neglecting any crossing angle.

III.4.3.2.3 Luminosity

At the LHC, the luminosity quoted for heavy-ion collisions is defined in the usual way. In other words it is the *nucleus-nucleus* luminosity. Occasionally, the *nucleon-nucleon* luminosity,

$$L_{\text{NN}} = A_1 A_2 L \quad (\text{III.4.15})$$

is quoted. It is relevant in comparisons of different colliding species (at electron-ion colliders, the electron-nucleon luminosity is commonly quoted).

III.4.3.3 Colliding nuclei with each other

III.4.3.3.1 Single beam limits

In principle, heavy-ion beams are subject to similar limits as other hadron beams.

Single-particle dynamics and optics are very similar for particles with the same magnetic rigidity. However heavy ions are slightly slower and, even in the LHC, require a small reduction of the RF frequency to make them circulate on the same closed orbit.

Single-beam collective instabilities, including electron-cloud effects, are generally weaker than for protons since the charge per bunch is lower. The same goes for conventional beam-beam effects although there is a whole new class of beam-beam interactions arising from nuclear physics. In particular, luminosity lifetimes are short because of very large electromagnetic cross-sections due to the high nuclear charge.

The phenomenon of *intra-beam scattering*, that is, multiple small-angle Coulomb scattering within particle bunches, is a very strong source of emittance growth for the lead beams in the LHC. However, the basic theory is not covered in the introductory JUAS courses, so we shall not discuss it here. Similarly, the extremely important topic of *beam collimation* would require an extensive introduction and explanation of how it is significantly more complicated than the proton case, so we shall confine ourselves to a few remarks in passing.

III.4.3.3.2 Synchrotron radiation

As we have seen above, the mass of the $^{208}\text{Pb}^{82+}$ nucleus compared to the proton mass $m_{\text{Pb}} = A_p m_p = 206.43 m_p$ and its energy is $E_{\text{Pb}} = Z E_p = 574 \text{ TeV}$ at the design magnetic field of the LHC. As a consequence, the wavelengths of the synchrotron radiation emitted by the Pb ions at top energy in the LHC are in the ultraviolet range.

Since this is far larger than the nuclear radius, the $Z = 82$ charges of the nucleus will radiate coherently like a single charge.

Comparing the radiation damping times, τ , for a Pb nucleus and a proton in the same ring (i.e., in the same magnetic field) shows that

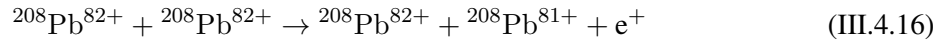
$$\frac{\tau_{\text{P}}}{\tau_{\text{Pb}}} = \frac{Z^5}{A_p^4} \approx 2.04,$$

Somewhat surprisingly, the radiation damping for heavy ions is *twice as fast* as for protons *in the same magnetic ring*.

At the LHC design energy, the longitudinal radiation damping time $\tau_{\text{Pb}} \approx 12.7$ h, which is comparable to the IBS growth times for the design bunch intensity and will have a beneficial impact on luminosity performance and beam losses, particularly as the bunch intensity decays.

III.4.3.3.3 Secondary beams from the interaction points

Among the many processes induced by the intense photon fields in ultraperipheral collisions of Pb nuclei, bound-free pair production (BFPP)



creates a secondary beam of $^{208}\text{Pb}^{81+}$ with a fractional rigidity change $\delta = 0.01235$ that impinges in the dispersion suppressor. This process has the largest visible cross section at the LHC $\sigma \simeq 280$ b.

The $^{208}\text{Pb}^{81+}$, a one-electron, hydrogen-like ion emerging from these collisions has almost the same momentum but a smaller charge than the original nucleus and is therefore bent less in the magnets of the LHC. It constitutes a secondary beam emerging from the collisions that eventually impinges on the beam pipe, potentially depositing energy in the coils of a superconducting magnet. With the LHC luminosity, this beam can carry over 100 W of power and could potentially quench a superconducting magnet, bringing operation to an immediate stop. It can thereby impose a direct limit on luminosity.

Other secondary beams are produced when photonuclear interaction cause electromagnetic dissociation of one or more neutrons from the nucleus, creating $^{207,206,\dots}\text{Pb}^{82+}$ and other nuclei. These processes have comparable cross-sections.

III.4.3.4 Colliding protons with nuclei

The two-in-one design of the LHC's main magnets impose equal magnetic rigidities of the beams in the two apertures—if they are to stay on the same central orbits. They will then have unequal revolution frequencies, with Pb beams making eight fewer turns of the ring per minute than protons. This necessitates different RF frequencies for p and Pb ions during injection and accelerations, since the radial offsets required for equal frequencies would be too large to fit into the beam pipe. Moving beam-beam encounters are created that lead to modulations in the long-range beam-beam interaction strengths and phases. There were initial doubts as to the feasibility of this mode of operation. Thanks to large enough separation, cancellation effects along the interaction regions and the large magnetic rigidity it turned out that these effects are not severe at the LHC.

III.4.3.5 The LHC heavy-ion programme so far

This section provides a brief summary of the first decade of heavy-ion runs at the LHC (Run 1 and Run 2). More detailed accounts with abundant references can be found in [4–6] Projections of future performance beyond Run 2 are benchmarked against the performance achieved so far in [8].

III.4.3.5.1 *New operational paradigm*

An important difference between the present generation of hadron colliders and their predecessors is the operational paradigm.

The previous p–p, p– \bar{p} and, indeed, also e^+e^- and e–p colliders were dedicated, most of the time, to optimised steady luminosity accumulation at the highest energy. Conditions generally changed only slowly as the operators fine-tuned their parameters. Colliding multiple hadronic species, often at specific energies, introduces a third dimension beyond energy and luminosity. In the case of the LHC, the schedule requires recommissioning of a new collision configuration, its validation for the strict requirements of machine protection, an intensity ramp-up and a period of physics data-taking, all within a month. It is hardly possible to identify periods of steady operation in these runs as new ways to improve performance are brought in, almost day-by-day. As experience grew, the runs have piled on complexity with multiple variations of the configuration to meet experimental requirements within the same time frame. For example, the LHC is required to make reference p–p, p–Pb and Pb–Pb runs at the same centre-of-mass energy *per colliding nucleon pair* $\sqrt{s_{\text{NN}}} = \sqrt{Z_1 Z_2 / A_1 A_2} \sqrt{s_{\text{pp}}}$ (for colliding species $(Z_{1,2}, A_{1,2})$), to elucidate the emergence of collective behaviour in the multi-nucleon systems.

III.4.3.5.2 *A typical heavy-ion run*

In the early days of Run 1, the optical configurations used for the heavy-ion runs were very close to those used for protons. Since then they have diverged to an increasing degree, culminating in the 2018 run where the optics differed already in the combined ramp and squeeze. The preparation of the LHC cycle for a heavy-ion run is broadly similar to that of protons. Nevertheless, important details that are specific to heavy-ion operation can be particularly challenging. Owing to the short run time and complexity, planning of the set-up is crucial. Any delay, such as downtime of a day or so, has significant impact on the final luminosity. The typical procedure to prepare the heavy-ion cycle can be outlined as follows:

- Commissioning of new optics with protons;
- First injection of ion beams;
- Settings clean-up with beam through the cycle from injection until collisions;
- Machine protection validation: loss maps⁴ and asynchronous dumps at various stages throughout the cycle.

This initial phase takes about 3–4 days. Once the cycle is established, the following items constitute the data-taking phase of the run. No changes to the operational cycle are possible from this point (until the later re-validation).

During the run, further changes and special activities have to be included:

- Intensity ramp-up in physics;
- Luminosity production;

⁴A loss map is an excitation of a safe low-intensity beam to study the generic distribution of beam losses around the ring and ensure that no sensitive elements are exposed.

- Van der Meer scans with normal physics optics and nominal beam (Usually one experiment executes its scan programme, while the others remain in physics data taking mode);
- Reversal of the ALICE muon-spectrometer dipole polarity (involves a change of external crossing angle and thus optics settings);
- Machine protection re-validation after polarity reversal (if not done during initial commissioning phase);
- Another intensity ramp-up in physics;
- Luminosity production;
- A small number of essential “machine development” experiments spread over the run period.

All physics data are usually taken within about three weeks. In contrast to p–p, almost every other fill features a different configuration. Frequent changes in number of bunches and filling schemes throughout each run resulted in steady performance gains, often until the last fill of the run. The overall time is too short to truly reach a phase of stable operation.

Table III.4.1 summarises the principal parameters for Pb–Pb operation, from the initial LHC design values to the future upgrade values in the “HL-LHC” phase. Note that all the HL-LHC upgrades relevant for heavy-ion operation were completed by the start of Run 3 in 2022.

III.4.3.5.3 *First Pb–Pb runs in 2010 and 2011*

Commissioning of the first Pb–Pb collisions at the reduced beam energy of 3.5 Z TeV in 2010 followed a cautious approach, exploiting the principle of equal magnetic rigidity to re-establish the orbit and identical optics of the preceding p–p run. The only change was the reduction of the crossing angle to zero in the ALICE experiment, with opening of the tertiary collimators, to allow unimpeded passage of spectator neutrons to the zero-degree calorimeters (ZDCs). Following RF capture with modified frequency and the necessary series of collimation loss-map validations at the main steps of the magnetic cycle, first collisions were established within four days and performance was ramped-up rapidly in the following days.

This run showed the importance of very carefully crafted commissioning plans, the extraordinary reproducibility and reliability of the LHC hardware and the maturity of operating procedures and controls. Numerous concerns about the feasibility of heavy-ion operation were laid to rest and there was an immediate harvest of significant physics results.

In the second Pb–Pb run at 3.5 Z TeV, several improvements were made: longer trains of bunches were injected, the optics was modified to provide $\beta^* = 1$ m in ALICE as well as ATLAS and CMS. This resulted in substantial spreads in the intensities and emittances of individual bunches along the trains. The integrated luminosity over the run was increased by more than an order of magnitude.

III.4.3.5.4 *The first p–Pb runs*

A feasibility test of unequal frequency injection, ramping and a prototype of the cogging process to equalise frequencies at top energy was performed in 2011. This led to a 16 h pilot physics run in 2012 and the unexpected discoveries of long-range correlations indicating collectivity in small systems. In

Table III.4.1: Representative simplified beam parameters at the start of the highest luminosity physics fills, in conditions that lasted for > 5 days, in each annual Pb–Pb run. The original design values for Pb–Pb collisions and future upgrade Pb–Pb goals are also shown (in this column the integrated luminosity goal is to be attained over the 4 Pb–Pb runs in the 10-year periods before and after 2020). Peak luminosities are averages for ATLAS and CMS (ALICE being levelled). The smaller luminosities delivered to LHCb from 2013–2018 are not shown. Emittance and bunch length are RMS values. The series of runs with $\sqrt{s_{\text{NN}}} = 5.02$ TeV also included p–p reference runs, not shown here. Design and record achieved nucleon-pair luminosities are boxed, and some key parameters related to p–Pb parameters in Table III.4.2 are set in red type, for easy comparison. The upgrade peak luminosity is reduced by a factor $\simeq 3$ from its potential value by levelling.

| Quantity | design | achieved | | | | upgrade |
|--|-----------|----------|------|-------------|-----------------|-------------------|
| Year | (2004) | 2010 | 2011 | 2015 | 2018 | ≥ 2021 |
| Weeks in physics | - | 4 | 3.5 | 2.5 | 3.5 | - |
| Fill no. (best) | | 1541 | 2351 | 4720 | 7473 | - |
| Beam energy $E[Z \text{ TeV}]$ | 7 | 3.5 | | 6.37 | 6.37 | 7 |
| Pb beam energy $E[A \text{ TeV}]$ | 2.76 | 1.38 | | 2.51 | 2.51 | 2.76 |
| Collision energy $\sqrt{s_{\text{NN}}} [\text{TeV}]$ | 5.52 | 2.51 | | 5.02 | 5.02 | 5.52 |
| Bunch intensity $N_b [10^8]$ | 0.7 | 1.22 | 1.07 | 2.0 | 2.2 | 1.8 |
| No. of bunches k_b | 592 | 137 | 338 | 518 | 733 | 1232 |
| Pb normalised emittance $\epsilon_N [\mu\text{m}]$ | 1.5 | 2. | 2.0 | 2.1 | 2.0 | 1.65 |
| Pb bunch length $\sigma_z [\text{m}]$ | 0.08 | | | 0.07–0.1 | | 0.08 |
| $\beta^* [\text{m}]$ | 0.5 | 3.5 | 1.0 | 0.8 | 0.5 | 0.5 |
| Pb stored energy [MJ/beam] | 3.8 | 0.65 | 1.9 | 8.6 | 13.3 | 21 |
| Luminosity $L_{\text{AA}} [10^{27} \text{cm}^{-2} \text{s}^{-1}]$ | 1 | 0.03 | 0.5 | 3.6 | 6.1 | 7 |
| NN luminosity $L_{\text{NN}} [10^{30} \text{cm}^{-2} \text{s}^{-1}]$ | 43 | 1.3 | 22. | 156 | 264 | 303 |
| Integrated luminosity/experiment $[\mu\text{b}^{-1}]$ | 1000 | 9 | 160 | 433,585 | 900,1800 | 10^4 |
| Int. NN lumi./expt. $[\text{pb}^{-1}]$ | 43 | 0.38 | 6.7 | 19,25.3 | 39,80 | 4.3×10^5 |

early 2013, the first full p–Pb run took place, gaining three orders of magnitude in luminosity in a few days. Operation included separate chromatic correction of the “off-momentum” collision optics, complex filling schemes to illuminate LHCb for its first participation in the heavy-ion programme, Van der Meer scans, low-luminosity minimum-bias running for the ALICE experiment, and manipulation of luminosity burn-off to equalise luminosity among the experiments. Reversal of the beam directions half-way through required a partial recommissioning and validation of the optics.

The evolution of the main parameters in the p–Pb runs to date is summarised in Tab. III.4.2 and the accumulation of integrated luminosity in Fig. III.4.1.

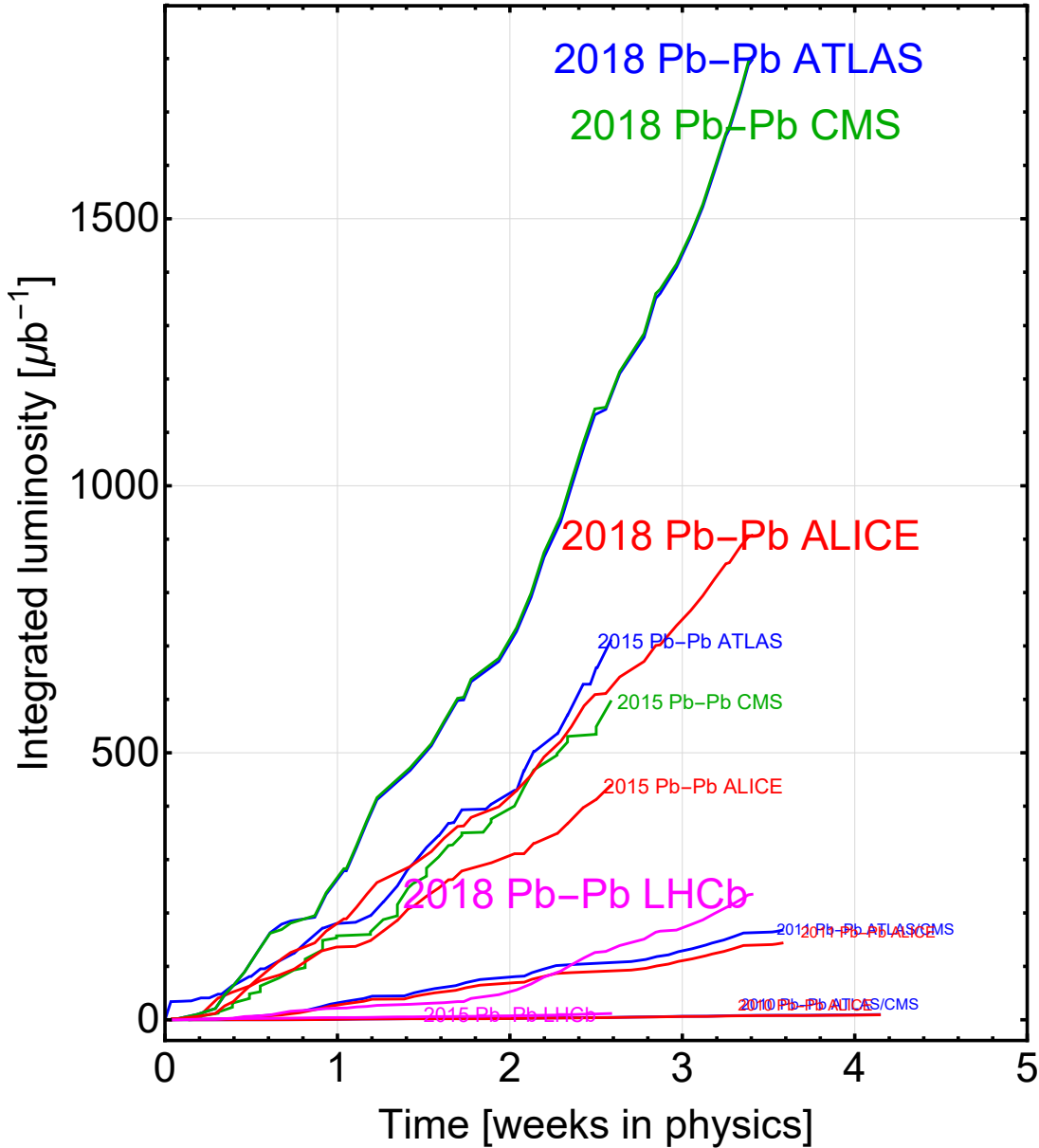


Fig. III.4.1: Accumulation of integrated luminosity in each LHC experiment in all Pb-Pb runs from 2010 to 2018, counted from the first declaration of Stable Beams.

III.4.3.5.5 Major steps for Pb-Pb in 2015

After its first long shutdown of the LHC, the magnetic fields of the LHC were increased to provide a beam energy of the proton beams in the LHC was increased to 6.5 TeV. However the Pb-Pb run took place at slightly lower magnetic fields, yielding 6.37Z TeV because this gave the same centre-of-mass energy per colliding nucleon pair, Eq. III.4.12, $\sqrt{s_{\text{NN}}} = 5.02$ TeV as in the p-Pb run of 2013, allowing direct comparison of data taken with the two types of collisions. The comparisons were completed with short p-p reference runs at the same $\sqrt{s_{\text{NN}}}$.

It is interesting to observe that the Pb-Pb collisions in 2015 were the first man-made collisions of any kind to exceed 1 PeV in total centre-of-mass energy, \sqrt{s} .

In the 2015 Pb-Pb collisions, the power of the secondary beams emitted from the interaction

Table III.4.2: Representative simplified beam parameters at the start of the highest luminosity physics fills, in conditions that lasted for > 5 days, in the one-month p–Pb runs . The very short pilot run in 2012 is not shown. The original “design” values for p–Pb collisions are also shown (in this column the integrated luminosity goal was supposed to be obtained over a few runs). Peak luminosities are averages for ATLAS and CMS (ALICE being levelled). The smaller luminosities delivered to LHCb from 2013–2016 and in the minimum-bias part of the run in 2016 are not shown. Emittance and bunch length are RMS values. Single bunch parameters for these p–Pb or Pb–p runs are generally those of the Pb beam. Design and record achieved nucleon-pair luminosities are boxed, and some key parameters related to p–Pb parameters in Table III.4.1 are set in red type, for easy comparison.

| Quantity | “design” | achieved | |
|--|--|--------------|---|
| Year | (2011) | 2012–13 | 2016 |
| Weeks in physics | - | 3 | 1, 2 |
| Fill no. (best) | | 3544 | 5562 |
| Beam energy $E[Z \text{ TeV}]$ | 7 | 4 | 4,6.5 |
| Pb beam energy $E[A \text{ TeV}]$ | 2.76 | 2.51 | 1.58,2.56 |
| Collision energy $\sqrt{s_{\text{NN}}} [\text{TeV}]$ | 5.52 | 5.02 | 5.02,8.16 |
| Bunch intensity $N_b [10^8]$ | 0.7 | 1.2 | 2.1 |
| No. of bunches k_b | 592 | 358 | 540 |
| Pb norm. emittance $\epsilon_N [\mu\text{m}]$ | 1.5 | 2. | 1.6 |
| Pb bunch length $\sigma_z [\text{m}]$ | 0.08 | 0.07–0.1 | |
| $\beta^* [\text{m}]$ | 0.5 | 0.8 | 10, 0.6 |
| Pb stored energy [MJ/beam] | 3.8 | 2.77 | 9.7 |
| Luminosity $L_{\text{AA}} [10^{27} \text{cm}^{-2} \text{s}^{-1}]$ | 150 | 116 | 850 |
| NN luminosity $L_{\text{NN}} [10^{30} \text{cm}^{-2} \text{s}^{-1}]$ | 43 | 24 | 177 |
| Integrated luminosity/experiment [μb^{-1}] | 10^5 | 32000 | 1.9×10^5 |
| Int. NN lumi./expt. [pb^{-1}] | 21 | 6.7 | 40 |

point by the BFPP process reached new levels while the propensity of the bending magnets to quench increased with the magnetic field. The BFPP beams emerging to the left and right of the ATLAS and CMS experiments, were carrying $P_{\text{BFPP}} \lesssim 80 \text{ W}$. This beam power is about 35 times greater than that contained in the luminosity debris and is focused on a specific location.

The 2015 run demonstrated a technique using orbit bumps to displace the BFPP losses safely into a connection cryostat that could be implemented in the optics around the ATLAS and CMS experiments, and so avoiding the risk of quenches. The question of the quench limit of the LHC main dipole magnets was finally resolved (after some 20 years of indirect estimations and discussion) in the first successful controlled quench test measurement at the LHC [7] which showed that the true level corresponded to the BFPP losses at about 2.3 times the Pb–Pb design luminosity.

To reduce the risk of quenches, orbit bumps around the impact locations at IR1 and IR5 were im-

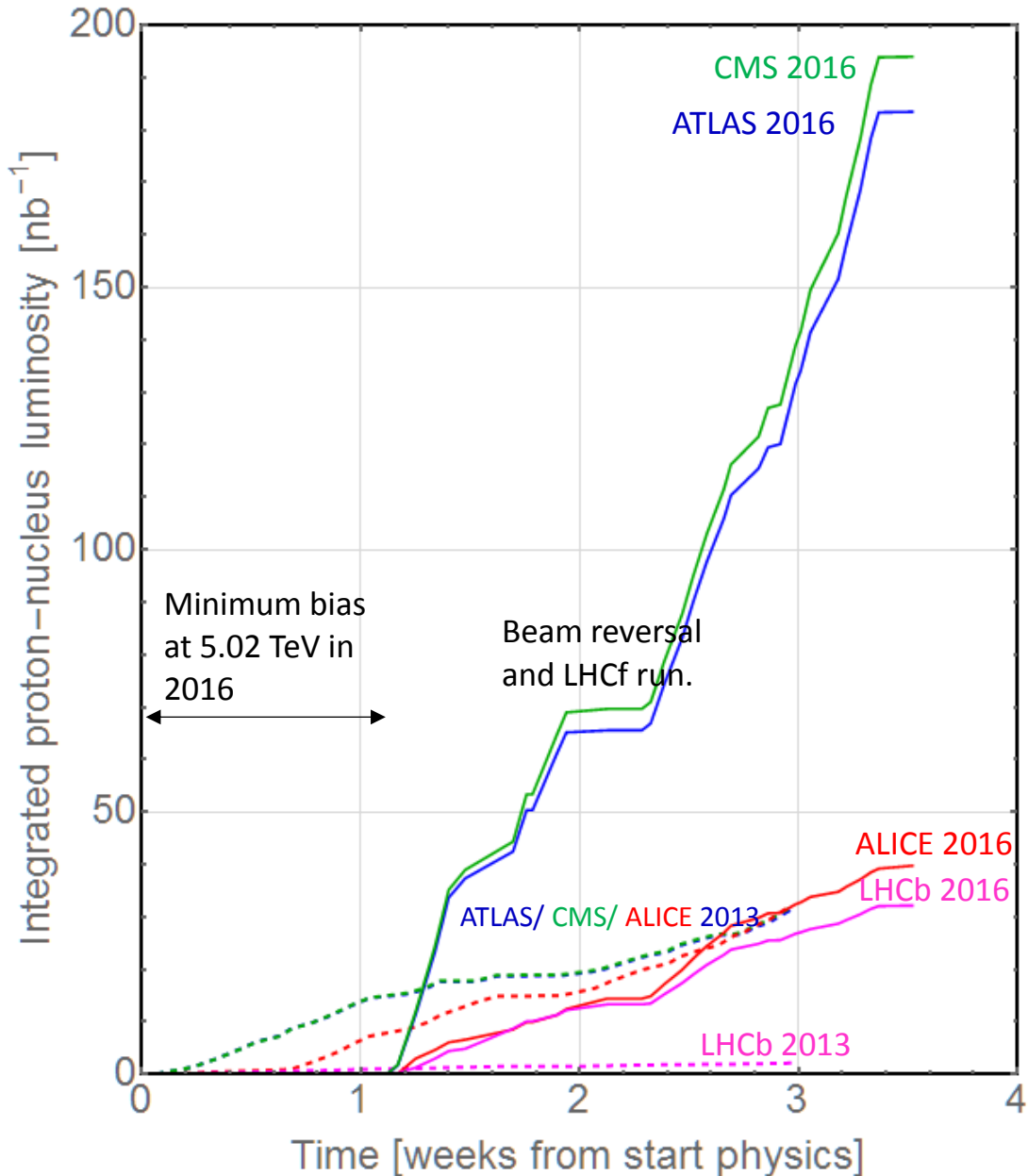


Fig. III.4.2: Accumulation of integrated luminosity in each LHC experiment in the p–Pb runs of 2013 and 2016, counted from the first declaration of Stable Beams.

plemented in order to move the losses out of the dipole and into the connection cryostat ("missing dipole" in the dispersion suppressor). Orbit bumps were also implemented at IR2. However, because of the opposite polarity of the quadrupoles the losses can not be moved into the connection cryostat around this IP. The bump served only to spread out these losses over the focusing quadrupole locations in two cells. Fortunately, at that time ALICE still required the luminosity to be levelled at $\mathcal{L}1.27$. The trajectories of the BFPP (red) and electromagnetic dissociation (EMD, green) beams are shown in Fig. III.4.3. These orbit bumps were used routinely for the first time throughout the entire run. No luminosity production fill was interrupted by a quench.

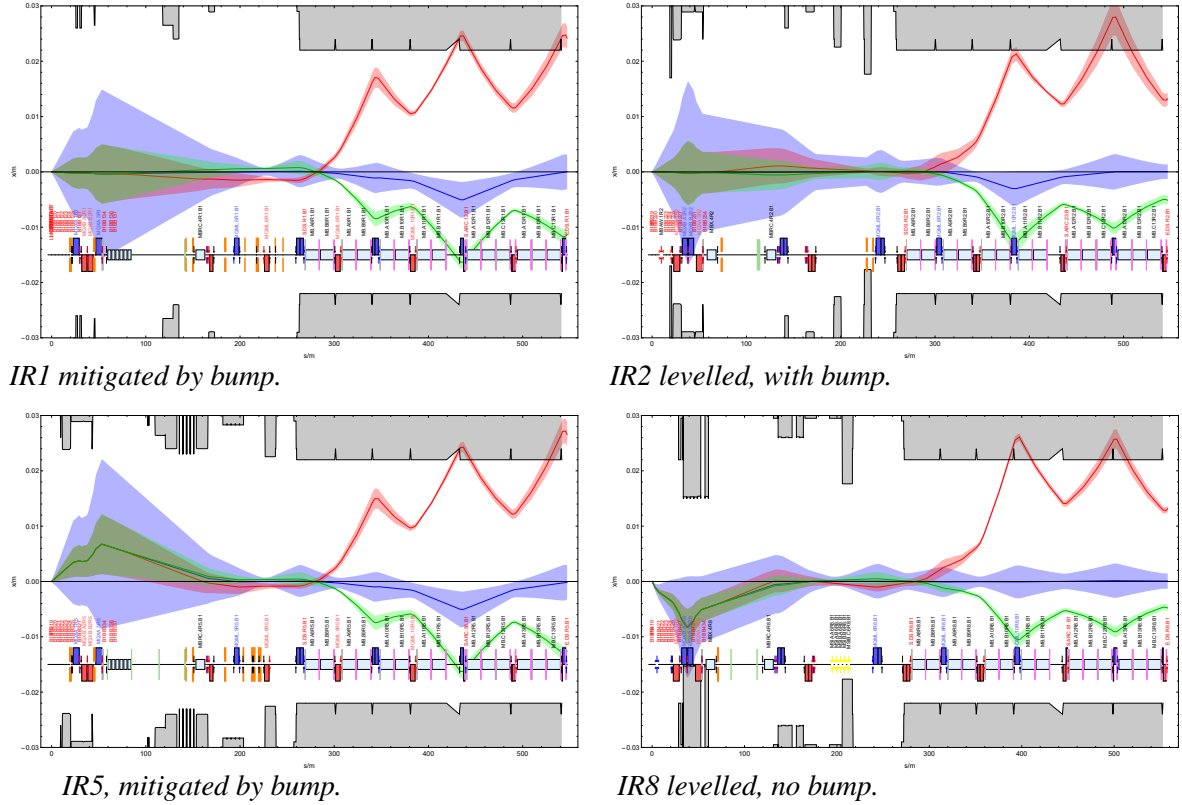


Fig. III.4.3: Calculated secondary beams from collisions in the four experiments. The 10σ main-beam envelope is shown in blue, and the 5σ BFPP and EMD secondary-beam envelopes are shown in red and green. Note that these beams are smaller than the main beam at the IP since their source is the luminous region but their size varies differently along the beam line because of chromatic effects. In IR1 and IR5 the orbit bumps displace the BFPP beam into the connection cryostat, allowing luminosity, $\mathcal{L} = 6.4 \times 10^{27} \text{ cm}^{-2}\text{s}^{-1}$ (in 2018), far beyond the quench level, $\mathcal{L} = 2.3 \times 10^{27} \text{ cm}^{-2}\text{s}^{-1}$ found in 2015. In IR2 the luminosity is levelled at the $\mathcal{L} = 1 \times 10^{27} \text{ cm}^{-2}\text{s}^{-1}$, the design and present saturation value of the ALICE detector but the risk of quenches is further mitigated with a bump that distributes the losses between two locations. In IR8 no mitigation was implemented but the luminosity was levelled at $\mathcal{L} = 1 \times 10^{27} \text{ cm}^{-2}\text{s}^{-1}$ (in 2018).

III.4.3.6 Multiple p–Pb conditions in 2016

The LHC experiments' requirements for the second p–Pb run in 2016 diverged. ALICE requested low-luminosity minimum-bias operation at the 2013 energy of 4 Z TeV while ATLAS and CMS requested maximum energy (6.5 Z TeV) and luminosity. A complex run scheme, based on the physics of beam lifetime, was proposed with an initial week in the ALICE conditions followed by two weeks in the ATLAS/CMS conditions. Further goals for all experiments, including LHCb and LHCf, were worked into the prioritised plan. The low-luminosity conditions allowed extremely long fills (up to a record 38 h) and an unprecedented 75% of time spent in Stable Beams. In the high-energy phase, luminosity approached six times the “design” value thanks to the implementation of synchronous operation of beam-position monitors allowed the proton-bunch charge to be increased beyond that of the Pb beam. In the end, all high-priority and most subsidiary physics goals were met.

III.4.3.6.1 The 2017 Xe–Xe run

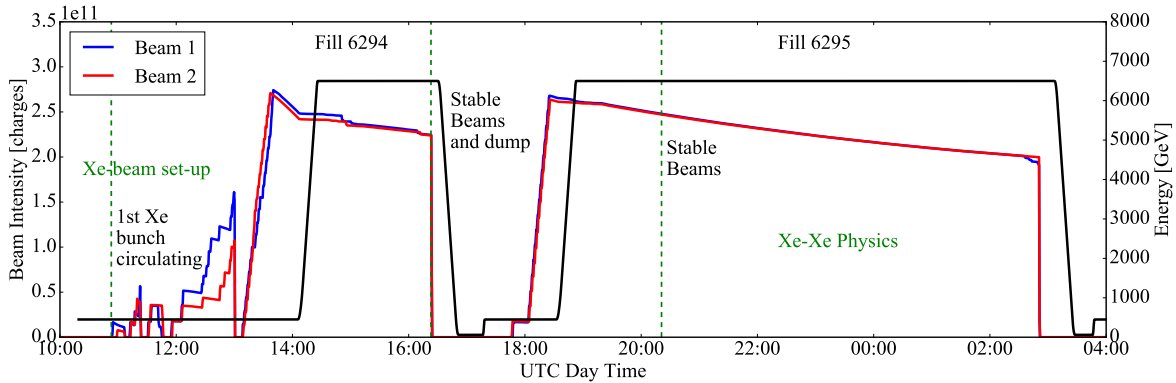


Fig. III.4.4: Evolution of the beam intensity (red and blue) and energy (black) throughout the Xe–Xe run.

Although no ion operation was foreseen in 2017 at first, the opportunity to bring xenon that was used in the injectors physics programme into the LHC was taken. Following the model of the first p–Pb run in 2012, on 12 October 2017, 16 h of beam time were dedicated to setting-up Xe–Xe collisions (see Fig. III.4.4 for an overview of the run). Rich physics output, which has served as reference comparison in the analyses of many of the later Pb–Pb runs, was harvested from the subsequent 6.5 h of Stable Beams. Results were reported by all LHC experiments, clarifying the transitions between Pb–Pb p–Pb and p–p. The results provided important input for possible future runs with lighter nuclei.

It was the first time the LHC circulated another species than protons or Pb and again illustrated its “beyond-design” potential. Also from the point of view of machine studies and understanding, the Xe operation was very valuable, especially for the collimation system cleaning measurements and simulation studies. Together with the similar pilot p–Pb run in 2012, it holds the record for the number of physics papers published per hour of beam time! Betatron cleaning efficiency was measured for the two beams and planes with the standard collimation setup and crystal collimation.

III.4.3.6.2 Pb–Pb in 2018: towards the heavy-ion goals of HL-LHC

The gradual divergence from operation with the machine configuration identical to p–pin 2010 culminated in 2018 with the commissioning of an entirely new cycle, including a parallel combined ramp-and-squeeze and squeeze down to $\beta^* = 0.5$ m in ATLAS, ALICE and CMS and to $\beta^* = 1.5$ m in LHCb, was designed and commissioned. The magnetic cycles for p–p and Pb–Pb only shared the injection conditions.

III.4.3.7 Optics

The Pb–Pb cycle for 2018 aimed for the smallest ever β^* in ALICE and LHCb. The combined ramp and squeeze (CRS) was redesigned, bringing β^* down to $\beta^* = (1, 1, 1, 1.5)$ m at IP1(ATLAS), IP2(ALICE), IP5(CMS) and IP8(LHCb), compared to $\beta^* = (1, 10, 1, 3)$ m at the end of the p–pramp. Then a short squeeze segment (4.5 min) at constant energy was enough to establish the target collision configuration $\beta^* = (0.5, 0.5, 0.5, 1.5)$ m, keeping LHCb constant, while reducing β^* by a further factor of 2 in the

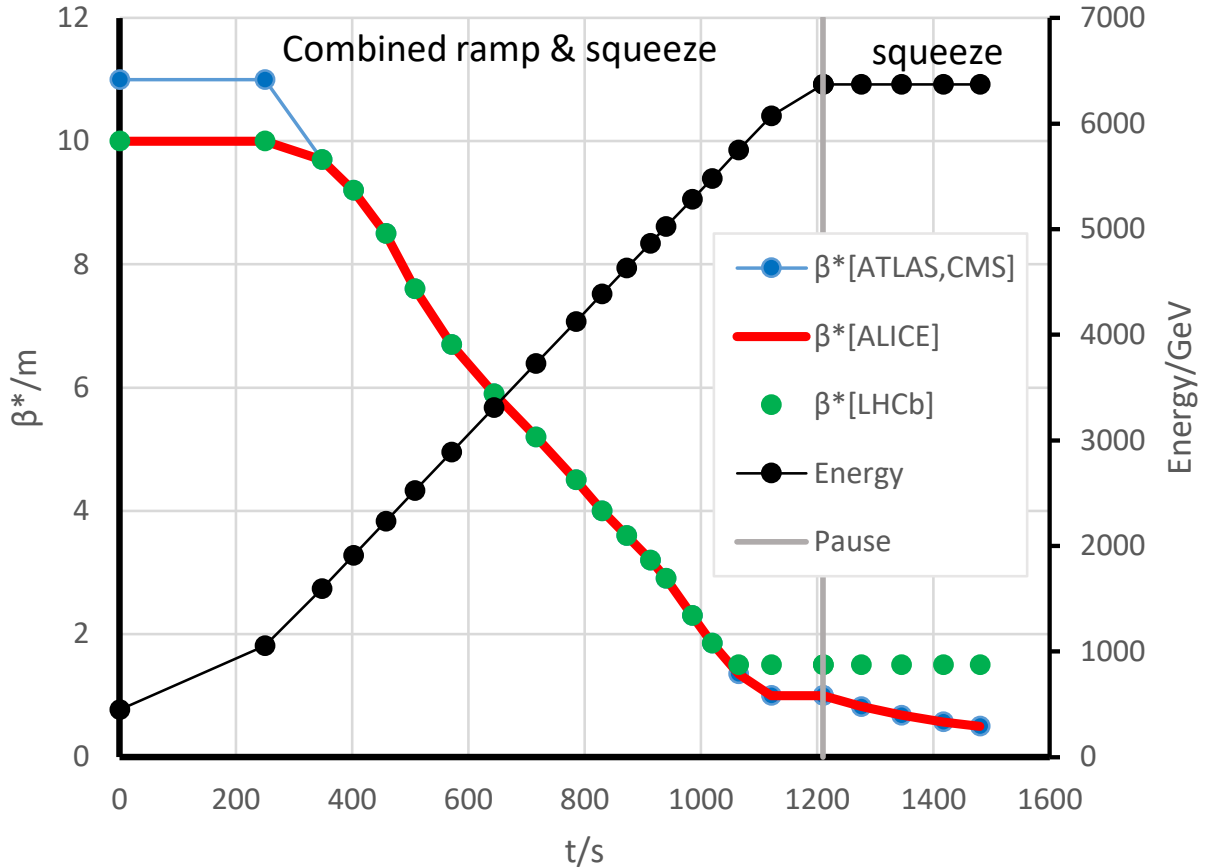


Fig. III.4.5: Timing structure of the CRS (left) and of the small squeeze segment at top energy (right) in terms of the β^* values at the experimental IPs. Changes of the multiple crossing-angle, separation and other orbit bumps are not indicated. Dots indicated fully matched two-ring optics.

other three experiments. Figure III.4.5 shows the efficient timing of these two beam processes (CRS and squeeze at collision energy).

The variously horizontal and vertical half-crossing angles in collision were brought to $160\ \mu\text{rad}$ in ATLAS and CMS, $\theta_b = 170\ \mu\text{rad}$ in LHCb, and $\theta_A \pm 137\ \mu\text{rad}$ in ALICE, where $\theta_A = 77\ \mu\text{rad}$ and $\theta_b = -150\ \mu\text{rad}$ are the angles generated by the internal spectrometer compensation bumps of ALICE and LHCb. The ALICE spectrometer polarity was reversed half-way through the run, requiring a passage of the external crossing angle through zero at the end of the squeeze. To reduce the associated risk, the horizontal separation was increased from 2 to 3 mm. As in 2015, the ALICE interaction point was lowered by 2 mm to compensate sinking of the experiment.

A major part of the preparation for this run was the adjustment of the collimation system and beam-loss monitor (BLM) thresholds for tolerable losses from the BFPP effect and also from collimation. Since the necessary background material has not been introduced in this course, we refer to [6] for further information and citations.

III.4.3.7.1 Lessons learned from 2018 Pb–Pb run

Preceding this run, optics commissioning was started with proton beams for about two shifts during p–p physics time. A fault of the ion source just a few days before the start of the ion operation led to a

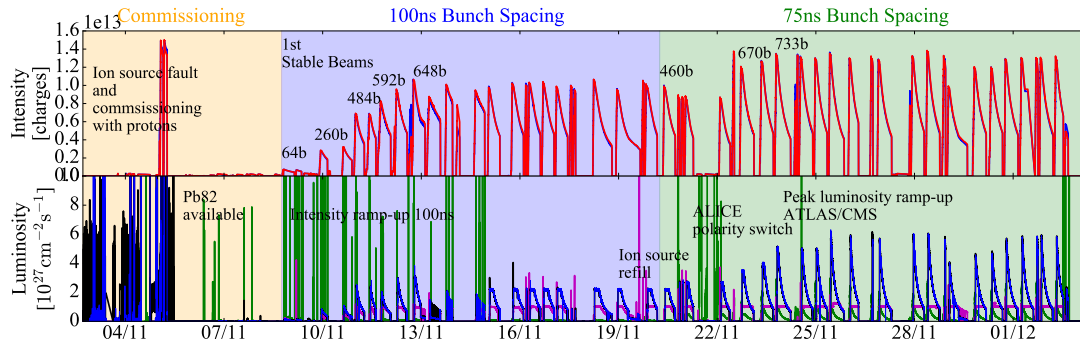


Fig. III.4.6: Run overview of beam intensity (top) and luminosity (bottom) through the 2018 Pb–Pb run. Periods of commissioning (yellow) and operation with 100 ns (blue) and 75 ns (green) bunch spacing are highlighted.

delay in the commissioning with ion beams after the technical stop and a degraded beam quality during the first week of the run. Commissioning was advanced with proton beams as far as possible and a requested repetition of the luminosity calibration for the proton special physics run at injection energy was performed in order to make best use of the time until Pb beam was available in the complex.

An initial problem with beam size in ALICE led to a reduced levelling time in the experiment in the first part of the run. The issue could be traced back to a settings error in the skew-quadrupoles used to correct the local betatron coupling in IR2. This was corrected during the re-validation after the ALICE polarity reversal for the second half of the luminosity data taking. Luminosity sharing strategies, including the re-optimisation of filling schemes to favour ALICE in number of colliding bunches and luminosity levelling in ATLAS/CMS, were applied to compensate for the lost ALICE luminosity. Additional checks have been developed to avoid this problem in future runs. It is advisable to plan set-up phases with just-in-time validations in order to be able to cope with such problems and perform re-validation steps.

During the second part of the run trains with an improved 75 ns bunch spacing and higher single bunch intensity became available. A new production scheme in LEIR splits the beam into three instead of two bunches that are transported through the PS and SPS without further splitting. Although it has been observed that these bunches are at the limit of stability in the SPS, they were the basis of an extra beam intensity boost in the LHC. This helped especially LHCb who could be provided with about an order of magnitude more colliding bunches. Because of this significant increase in peak luminosity in LHCb, the luminosity had to be levelled to $\mathcal{L} = 1 \times 10^{27} \text{ cm}^{-2} \text{ s}^{-1}$ (same as ALICE) to avoid quenches due to the absence of BFPP bumps (see Fig. III.4.3).

The luminosity levelling targets in IP1/5 were slowly increased fill-by-fill to finally reach a new peak luminosity record of $\mathcal{L} = 6.4 \times 10^{27} \text{ cm}^{-2} \text{ s}^{-1}$, almost twice the record set in 2015 and in reach of the HL-LHC specification. That provided an important validation of the BFPP bump mitigation strategy in IP1/5 for HL-LHC.

As can be seen from Tabs. III.4.1 and III.4.2 and Figs. III.4.1 and III.4.2, the peak luminosity goals for heavy-ion operation of the LHC have been exceeded by far and the integrated luminosity goals for the first phase of operation have been attained in less time than expected. Furthermore the peak luminosity

goals for heavy-ion operation at HL-LHC have almost been attained in ATLAS and CMS. It remains to sustain them for longer in order to accumulate the desired integrated luminosity.

III.4.3.8 The future of nuclear collisions at the LHC

The results from LHC heavy-ion operation so far have yielded new insights and precision measurements that motivate further extensions both in terms of luminosity and colliding species.

We refer the reader to [8] for a detailed account of simulations of future luminosity performance and their benchmarking against what was achieved in Run 1 and Run 2.

Future Pb–Pb and p–Pb operation will depend on upgrades to the LHC machine installed by the beginning of Run 3 in 2022. The upgraded ALICE experiment will be able to receive more than six times higher peak luminosity which will be enabled by the installation of special collimators around IP2 to absorb the powerful BFPP secondary beams.

A significant increase in beam intensity is required and should be provided by upgrades of the injectors. The original LHC collimation system will be unable to cope with the new level single beam losses. It will be upgraded to a system working with the new principle of crystal collimation.

A run with oxygen beams, in both O–O and p–O collisions is already foreseen and studies are underway for collisions of other lighter species in the years beyond 2030.

References

- [1] W. Fischer, J.M. Jowett, "Ion Colliders", *Reviews of Accelerator Science and Technology* Vol. 7 (2014) 49–76, World Scientific Publishing Company, [doi:10.1142/S1793626814300047](https://doi.org/10.1142/S1793626814300047).
- [2] P. Braun-Munzinger, V. Koch, T. Schäfer, and J. Stachel, "Properties of hot and dense matter from relativistic heavy ion collisions", *Phys. Rep.* 621, 76 (2016), [doi:10.1016/j.physrep.2015.12.003](https://doi.org/10.1016/j.physrep.2015.12.003).
- [3] W. Busza, K. Rajagopal and W. van der Schee, "Heavy-Ion Collisions: The Big Picture and the Big Questions", *Annu. Rev. Nucl. Part. Sci.* 2018. 68:339–76, [doi:10.1146/annurev-nucl-101917-020852](https://doi.org/10.1146/annurev-nucl-101917-020852).
- [4] J.M. Jowett, "Colliding Heavy Ions in the LHC," in *Proceedings, 9th International Particle Accelerator Conference (IPAC 2018): Vancouver, BC Canada, 2018*, p. TUXGBD2, 2018, [doi:10.18429/JACoW-IPAC2018-TUXGBD2](https://doi.org/10.18429/JACoW-IPAC2018-TUXGBD2).
- [5] J.M. Jowett, C. Bahamonde Castro, W. Bartmann, C. Bracco, R. Bruce, J.M. Coello de Portugal, J. Dilly, S.D. Fartoukh, E. Fol, N. Fuster-Martínez, A. Garcia-Tabares, M. Hofer, E.B. Holzer, M.A. Jebramcik, J. Keintzel, A. Lechner, E.H. Maclean, L. Malina, T. Medvedeva, A. Mereghetti, T.H.B. Persson, B.Aa. Petersen, S. Redaelli, B. Salvachua, M. Schaumann, C. Schwick, M. Solfaroli, M.L. Spitznagel, H. Timko, R. Tomás, A. Wegscheider, J. Wenninger, D. Wollmann, "The 2018 Heavy-Ion Run of the LHC", in *Proceedings of the 10th International Particle Accelerator Conference (IPAC2019): Melbourne, Australia, May 19-24, 2019* p. 225, 2019, [doi:10.18429/JACoW-IPAC2019-WEYYPLM2](https://doi.org/10.18429/JACoW-IPAC2019-WEYYPLM2).
- [6] J.M. Jowett, M. Schaumann, "Overview of ion runs during Run 2", in *Proceedings of the 9th LHC Operations Evian Workshop, Evian, France (2019)*, indico.cern.ch/event/7518570.

- [7] M. Schaumann, J. M. Jowett, C. Bahamonde Castro, R. Bruce, A. Lechner and T. Mertens, “Bound-free pair production from nuclear collisions and the steady-state quench limit of the main dipole magnets of the CERN Large Hadron Collider,” *Phys. Rev. Accel. Beams* **23** (2020), 121003, [doi:10.1103/PhysRevAccelBeams.23.121003](https://doi.org/10.1103/PhysRevAccelBeams.23.121003).
- [8] R. Bruce, M.A. Jebramcik, J.M. Jowett, T. Mertens and M. Schaumann, “Performance and luminosity models for heavy-ion operation at the CERN Large Hadron Collider,” *Eur. Phys. J. Plus* **136** (2021) no.7, 745, [doi:10.1140/epjp/s13360-021-01685-5](https://doi.org/10.1140/epjp/s13360-021-01685-5).